ACID ATTACK IN A CONCRETE SEWER PIPE - A PETROGRAPHIC & CHEMICAL INVESTIGATION

Dipayan Jana[1] and Richard A. Lewis[2]

[1] Dipayan Jana, P.G., Construction Materials Consultants, Inc. Greensburg, PA 15601
[2] Richard A. Lewis, P.E., Openaka Corporation, Inc., Denville, NJ 07834

ABSTRACT

A 30-in. diameter steel cylinder reinforced concrete pipe (concrete pressure pipe, bar-wrapped, steel-cylinder type, AWWA C303) was investigated for deterioration by sulfuric acid generated inside the sewage force main. A section of the pipe from the crown region, containing a mortar coating, steel cylinder, and mortar liner, was examined. Results show an inherent dense, low-absorptive, and impermeable nature of the outer coating but a soft, porous, and absorptive nature of the inner liner. The latter was severely attacked by sulfuric acid, lost 25 percent of its thickness, and developed distinct compositional and microstructural features typical of a sulfuric acid attack. The study emphasizes the importance of a dense, low water-cement ratio (*w/c*), and impermeable liner material for resisting such an attack in sewer pipes.

INTRODUCTION

The most common type of damage in concrete sewer pipe is corrosion of the pipe wall by sulfuric acid generated within the pipe (1). The first stage of such deterioration is the formation of hydrogen sulfide (H_2S) gas by decomposition of sulfur compounds; and, conversion of sulfates into sulfide by the sulfur-reducing, anaerobic bacteria situated in sewage effluent (slime) in the submerged portion (Figure 1). The H_2S gas diffuses through the sewage, escapes upward into the atmosphere above the effluent, dissolves into the moisture film that coats the above-sewage portion of the pipe wall, and becomes oxidized very rapidly to dilute sulfuric acid (H_2SO_4) by the aerobic, sulfur-oxidizing bacteria (e.g., thiobacillus) that colonizes at the exposed arch or crown of the pipe (2). Sulfuric acid then attacks and dissolves paste from the crown and portion of the wall-surface above the sewage. Acid attack causes preferential leaching of paste relative to the siliceous aggregates and corrosion of the inner wall of the pipe. The severity of corrosion depends on several inter-related factors such as the sulfur content of the effluent, the rate and amount of H_2S gas generation, the type and concentration of bacteria causing the H_2S-to-H_2SO_4 conversion, sewage temperature, pH, and the flow rate of the effluent (2, 3). The present paper describes the effect of microbial induced corrosion by sulfuric acid attack and the overall microstructural features of one such pipe.

Carbon dioxide gas in the sewer atmosphere causes carbonation along the inner wall of the pipe, which reduces the pH and creates an environment favorable for bacterial

growth. Thiobacillus does not grow until the inherent high pH (11 to 13) of the mortar is reduced down to 9 by carbonation. CO_2 and H_2S dissolved in moisture cause carbonation and promote bacterial growth. H_2S-to-H_2SO_4 conversion by thiobacillus and acid attack causes further reduction of pH of the liner. The concentration of dissolved H_2S in the moisture film increases significantly with decreasing pH (e.g., from 9.1 percent at a pH of 8 to 91 percent at a pH of 6). The type of thiobacillus colonization also depends on the pH of the liner - at an extremely low pH of 1 the most acidophilic type *thiobacillus concretivorous* forms, which is Latin for "concrete eaters" (4). Field investigations of several sewers show that the most severe damage occurs at the crown where the most acidophilic type of thiobacillus colonizes. The pH of the moisture film at the crown is 1 or 2 while the sewage is neutral.

The most common product of sulfuric acid attack is formation of calcium sulfate dehydrate, or gypsum, which occurs (sometimes intermixed with ettringite) as a white layer on the outer convex arch of the liner. Gypsum usually occurs as a white mass on the inner aerated surface of the liner and acts as a protective shield to the interior pipe from further penetration of acid. Intermittent high flow sometimes washes gypsum out and exposes the surface for further acid attack. In this case study, however, massive gypsum precipitation as a white layer occurred at the outer surface of the liner, i.e., at the liner-steel interface; the inner wall was severely leached out without any evidence of gypsum – this indicates severe leaching of the liner surface by acid, migration of sulfate solutions through the liner, and precipitation of gypsum-ettringite at the outer surface. The brownish yellow color of the corroded surface of the inner wall is due to direct oxidation of hydrogen sulfide to elemental sulfur and leaching of ferruginous components of aggregates.

This article describes a case study on sulfuric acid attack in the mortar liner of a sewer pipe, which has caused severe deterioration of the inner wall of the liner and spectacular development of gypsum and ettringite deposits on the outer wall of the liner. The attack, though resembling a classical sulfate attack, was initiated by the sulfuric acid inside the sewer.

CASE STUDY

A 30-in. diameter (0.75 m) steel cylinder reinforced concrete pipe (concrete pressure pipe, bar-wrapped, steel-cylinder type, AWWA C303[1]) was investigated for such attack. The pipeline consisted of an outer specified 1 in. thick mortar coating, a series of $^{7}/_{32}$-in. diameter reinforcing bars wrapped on a 1/8 in. thick steel cylinder, and an inner ½ to ¾ in. thick mortar liner inside the steel cylinder. Saw-cut sections of the pipe were col-

[1] American Water Works Association, AWWA C 303, "Standard for Concrete Pressure Pipe, Bar-Wrapped, Steel-Cylinder Type"; Denver, Colorado.

lected from a station (25+95) for laboratory analyses (Figures 2, 5, and 6). The mortar coating was unaffected by the exterior soil but the inner surface of the liner was severely corroded with a 25 percent loss of the total thickness and severe leaching of paste. The mortar coating, steel cylinder, and mortar liner, though mated to each other, were received in de-bonded conditions.

Laboratory examinations were done to determine the composition, overall quality, effect of acid attack on the mortar liner, condition of reinforcing bars in the coating, and the chloride-sulfur-sulfate profiles. Studies include: (a) petrographic examinations according to ASTM C 856, "Petrographic Examination of Hardened Concrete"; (b) chloride analyses according to ASTM C1152, "Acid-Soluble Chloride in Mortar and Concrete"; (c) water absorption according to ASTM C 642, "Specific Gravity, Absorption, and Voids in Hardened Concrete"; (d) sulfate analyses according to ASTM C 114, “Chemical Analysis of Hydraulic Cement”; (e) total sulfur analyses by the LECO method; (f) x-ray diffraction analysis; and (g) scanning electron microscopical examinations with energy-dispersive x-ray microanalysis (SEM-EDS). The last two methods were used for detecting the secondary deposits in the mortar liner. For the coating and liner, freshly fractured sections, finely ground sections, thin-sections, and several oil immersion mounts were prepared for detailed petrographic examinations. Samples for chloride, sulfate and total sulfur analyses were collected from successive depths of the coating and liner by dry drilling.

MORTAR COATING

The mortar coating is $1\frac{1}{4}$ in. in maximum thickness (Figure 2). The outer surface, in contact with soil, is rough, grayish brown, weathered, and covered with loose soil and sand particles. The inner surface, in contact with the steel cylinder, is smooth, formed, dark gray, and contains parallel, embedded, reinforcing bars having nominal diameters of $\frac{7}{32}$ in. and regular center-to-center spacing of $1\frac{5}{8}$ in. to $1\frac{1}{4}$ in. The reinforcing bars were not corroded. The reinforcing bar-cast surfaces contain neat paste having a thickness of $\frac{1}{64}$ in.

Aggregate – The mortar coating is dense, well consolidated, and made using well-graded, well-distributed natural siliceous – calcareous sand aggregate having a nominal maximum size of $\frac{1}{8}$ in. Sand particles are clear, light to medium gray, moderately dense, moderately hard, subangular to subrounded, fresh, uncracked, unaltered, uncoated and contain following various lithologies: oolitic, porous, arenaceous, argillaceous and dolomitic limestones, quartzite, granite, chert, greywacke, ferruginous and calcitic sandstones, opaque iron oxides, quartz, and feldspar. Sand particles are well graded, well distributed, and have been sound during their service in the coating.

Paste – Paste is dark gray, dense, hard, and firm. Freshly fractured surfaces have subconchoidal fractures and subtranslucent vitreous lusters. Residual and relict cement particles are abundant and are estimated to constitute 20 to 25 percent of the paste volume. The calcium hydroxide component of cement hydration occurs as small, platy and patchy units, uniformly dispersed in the paste, and are estimated to constitute 6 to 8 percent of the paste volume. Hydration of the portland cement is normal.

The reinforcing bar casts to depths of $^{1}/_{64}$ in. are neat pastes that are denser and darker than the paste elsewhere. The compositional and textural features of the paste are indicative of *w/c* estimated to be 0.34, except in the dark neat paste in the reinforcing bar cast surfaces that has an estimated *w/c* of 0.32 or less.

Carbonation – Carbonation has extended to a shallow depth of $^{1}/_{32}$ in. from the outer surface, and, in areas around the irregular voids up to the mid-depth location. The neat paste around the reinforcing bars is not carbonated. The bottom surface of the coating, at the haunch level of the reinforcing bars, is not carbonated. The shallow depth of surface carbonation is an indication of the dense nature of the coating.

Air – The coating contains some air voids that occur as irregularly shaped voids having a nominal size of $^{1}/_{32}$-in. The voids are more concentrated at the haunch level on two sides of the reinforcing bars. The air content is estimated to be 4 to 5 percent. The mortar coating is non-air-entrained.

Secondary Deposits – Fibrous and acicular crystals of ettringite are present as white secondary deposits in the voids in the bottom portions of coating. On reinforcing bar cast surfaces are white to light gray, thin, continuous deposits of calcium hydroxide and, to a lesser extent, ettringite.

Reinforcing bars – The reinforcing bars are intimately bonded to and embedded within the coating along its base. Reinforcing bars are fresh, clean and, as mentioned, without any trace of corrosion products.

Chloride Profile – Despite the absence of corrosion of the reinforcing bars, the mortar coating was analyzed for chloride contents at various depths to determine the chloride levels and any possibility for future corrosion. Figure 9 shows the sample locations and chloride contents at each depth. Samples adjacent to reinforcing bars were taken by dry drilling of neat paste in the bar-cast surfaces. The chloride contents increase from 0.014 percent at the bottom to 0.035 percent at the top. The profile is indicative of the introduction of chloride from the mortar-making ingredients and a portion contributed from the environment (i.e., from soil and groundwater above the pipe) that has penetrated into the coating. In the neat-paste in bar-cast surface, the chloride content is 0.032 percent, which is comparable to the value in the top. Such a high chloride is due to the absence of aggregates in the neat paste. All chloride contents are reported as percent by mass of the mortar. Despite the somewhat high chloride, the absence of corrosion of reinforcing

bars is largely due to the dense, low-absorptive, and impermeable nature of the mortar coating and the absence of oxygen to cause the corrosion.

Absorption, Volume of Permeable Voids – The 24-hour cold water-absorption of the mortar coating is 3.6 percent; the volume of permeable voids is 10.8 percent. The results are given in Table 1. The values are typical of a dense, low-absorptive coating.

Table 1 - Absorptions, specific gravities, and volumes of permeable voids in the mortar coating and liner.

Sample	Coating/ Liner	Absorption (%)		Specific Gravity				Volume of Permeable Voids (%)
		24-hour	5-hr. Boil	Bulk Dry	After 24-hour Absorption	After 5-hr. Boil	Apparent	
25+95	Coating	3.6	4.7	2.3	2.4	2.4	2.6	10.8
	Liner	7.4	7.5	2.2	2.4	2.4	2.7	16.8

Figure 7 shows the microstructural profile of mortar coating in thin-section photomicrographs taken by using a petrographic microscope. Overall, the mortar coating is sound and does not show any evidence of deterioration or chemical attack from the environment.

STEEL CYLINDER

The arched section of the steel cylinder between the liner and the coating has a thickness of $^{3}/_{16}$ –in. and a lateral dimension of 8 in. × $7^{1}/_{4}$ in. Its convex outer surface, in contact with the mortar coating, was not corroded - it contains impressions of the reinforced reinforcing bars and associated mortars (Figure 6). The inner surface in contact with the liner, however, has pitting corrosion at several small patches (Figure 6). The absence of corrosion in the outer surface but distinct pitting corrosion in the inside surface of the steel is indicative of: (a) a better quality of the mortar coating than the mortar liner in resisting the corrosive agents; and/or (b) migration of the agents of corrosion (chloride, carbonates, moisture, and oxygen) predominantly from the inner environment of the pipe through the mortar liner. The liner was more porous than the coating, which allowed ready movement of chemicals through the liner to the steel. Moreover, the erosion of the liner has reduced its thickness and helped ready access of corrosive agents to the steel.

MORTAR LINER

The mortar liner is arched, $^{9}/_{16}$ in. in nominal thickness and match-mated with the section of the steel cylinder. The outer surface, in contact with the steel cylinder is smooth, formed, light gray to bright white and contains a few small, patchy areas and pitted reddish brown corrosion products of steel cylinder at several locations. The inner surface is dark brown, severely weathered, leached, eroded with exposures of $^{1}/_{8}$-in. sized brown, weathered sand particles (Figure 8). A $^{9}/_{16}$ in. diameter hole at the center of the steel cylinder and extended into the liner was made to remove the sample (Figure 5).

Aggregate – Aggregate particles are $^{1}/_{8}$ in. in nominal maximum size and contain natural siliceous-calcareous sand. The aggregate has the following lithologies: limestone and its varieties (pure, fossiliferous, oolitic, porous, arenaceous), dolomite, chert, ferruginous chert (jasper), quartzite, granite, argillites, opaque iron ores showing shiny metallic luster, sandstone and its varieties (calcitic, argillaceous, ferruginous), siltstone, quartz sand, feldspar, mafic minerals. Particles are subangular to subrounded, fresh, uncracked, unaltered, and uncoated. Sand particles are well graded, well distributed, and have been sound during their service in the liner.

Paste – Paste is light gray to light brownish gray, and moderately soft to soft. Freshly fractured surfaces have subvitreous lusters and subconchoidal to subearthy textures. Residual and relict cement particles are few and estimated to constitute 6 to 8 percent of the paste volume. The calcium hydroxide component of cement hydration occurs as small, platy and patchy units uniformly dispersed in the interior, unaltered portions of the paste, and are estimated to constitute 8 to 10 percent of the paste volume. Hydration of the cement is normal. Fly ash, ground granulated blast furnace slag, and other mineral admixtures were not detected. The compositional and textural features of the paste in the interior, non-carbonated portions of the liner are indicative of a *w/c* estimated to be 0.50 ± 0.02.

Carbonation – Both the outer and the inner surface of the liner are severely carbonated. The interior of the liner is carbonated at varying degrees and locations. Carbonation of paste at the steel-liner interface has reduced the alkalinity (pH~9) of the liner and promoted corrosion of the inner surface of the steel cylinder.

Air – Air occurs as a few irregularly shaped voids having a nominal maximum size of $^{1}/_{64}$ in. The air content is estimated to be less than 1 percent. The liner is non-air-entrained.

Secondary Deposits – Secondary deposits are present all throughout the mortar liner – (a) as a thin, white layer of secondary ettringite, thaumasite, and gypsum on the outer surface of the liner, (b) acicular and fibrous ettringite in voids within the paste and along aggregate-paste interfaces (Figure 9), (c) matted thaumasite in voids near and at the out-

side surface of the liner, and (d) secondary calcium carbonate in voids throughout the mortar. These secondary compounds are indicative of exposure of the liner to moisture and sulfate-carbonate solutions for prolonged periods.

Sulfate Layer – Of special importance is the distinct white layer of secondary ettringite, thaumasite, and gypsum at the top surface of the liner that formed immediately beneath the steel cylinder. Such massive occurrence of sulfates as a distinct layer is the direct indication of sulfuric acid (sulfate) attack and the presence of abundant sulfate solution in the liner. Figure 4 shows x-ray diffraction analysis of this layer scraped from the surface – the abundance of gypsum and ettringite has decreased significantly at the mortar liner surface immediately beneath the white layer. Oil immersion mounts of white layer show intermixed fibers of secondary ettringite and thaumasite (the latter occur due to the presence of sulfate, carbonate, and cold temperature inside the pipe).

Chloride Profile – Similar to the coating, the liner was analyzed for chloride contents at various depths. Samples were obtained from the top, middle, and bottom portions of the liner (Figure 9); the top portion includes the white coat on the exposed surface and the bottom portion includes the brown, leached paste at the inside surface. The chloride contents are 0.044 percent at the top, 0.036 percent in the middle and 0.014 percent at the bottom. The profile is indicative of an upward migration of chloride-containing solutions through the liner (as well as some leaching of chloride at the inside wall).

Sulfate Profile – The mortar liner was also analyzed for sulfate (SO_3) and total sulfur. The top (excluding the outside white coat), middle, and bottom (including the inside surface) of the liner were separately analyzed. The respective sulfate contents are 1.65 percent at the top, 1.78 percent in the middle, and 1.46 percent at the bottom (Figure 9). The total sulfur contents are 1.34 percent at the top, 0.92 percent in the middle, and 0.76 percent at the bottom. The lowest sulfate and sulfur concentrations at the bottom are consistent with leaching of the paste by sulfuric acid. The sulfate and total sulfur contents are both indicative of sulfuric acid (sulfate) attack in the liner.

Absorption, Volume of Permeable Voids – The 24-hour water-absorption of the liner is 7.4 percent; the volume of permeable voids is 16.8 percent. The results are given in Table 1. The absorption and the volume of permeable voids are significantly higher than the corresponding values in the coating, indicating the more porous and permeable nature of the liner.

Table 2 provides the similarities and differences in compositional properties of the mortar coating and mortar liner.

Table 2 – Some properties of the mortar coating and liner described in the paper

Properties	Mortar Coating	Mortar Liner
Thickness	1¼ in.	9/16 in.
Outer surface	Exposed, Brown, Weathered	Smooth, White layer
Inner surface	Formed, Gray	Corroded (leached), Brown with exposed sand
Aggregates	Siliceous-Calcareous sand	Siliceous-Calcareous sand
Paste	Dense, hard, dark gray, portland-cement paste	Soft, porous, light gray, portland cement paste
Bulk estimated *w/c*	0.34	0.50
Water-absorption (24-hour, %)	3.6	7.4
Volume of permeable voids	10.8 percent	16.8 percent
Air Content	Non-air-entrained (4 to 5 percent)	Non-air-entrained (<1 percent)
Loss of thickness	Negligible	25%
Chloride content (average, % by mass of mortar)	0.026 percent; High chloride at the top	0.031 percent; High chloride at the top

Figure 8 shows the microstructural profile of mortar liner in thin-section photomicrographs taken by using a petrographic microscope.

EVIDENCES OF ACID ATTACK IN THE MORTAR LINER

There are four distinct microstructural evidences of sulfuric acid attack in the mortar liner:

(1) Corrosion of the liner – The nominal thickness of the liner is 9/16 in., which is 75 percent of the reported 'original' nominal thickness of 3/4 in. Thus, there is a 25 percent loss of the thickness of the mortar liner.

(2) Differential leaching of paste and carbonate aggregate relative to the siliceous aggregate – Significant leaching of the paste had occurred from the inner surface of the liner, which had exposed the aggregate particles. Siliceous aggregate particles (e.g., quartz

sand) are more sound and durable during leaching and stood prominently against the leached paste, whereas carbonate aggregate particles are less durable and showed evidence of acid erosion. The yellowish brown stain of the inner surface (Figure 3) is from the leached ferruginous components of the aggregates.

(3) Gypsum and Ettringite/Thaumasite Formation – As mentioned before, XRD analyses of the white layer on the outside surface of the liner detected gypsum, ettringite, and thaumasite (Figure 4). Also detected are some very fine, secondary calcite, and dolomite crystals. Such crusts of gypsum, ettringite and thaumasite indicate migration of sulfate and carbonate ions through the liner into the steel-liner interface. Figure 9 shows oil immersion mount of inter-grown mixture of ettringite and thaumasite in the white layer, and thin section photomicrograph of secondary ettringite precipitation along an aggregate-paste interface. Figure 10 shows SEM-EDS spectra of gypsum and ettringite from the white layer. Unlike other mechanisms of concrete deterioration, such as delayed ettringite formation, these ettringite occurrences indicate a slow leaching and decay of the liner without any noticeable expansion. There is no evidence of microcracking or so-called "gaps" around the aggregates to indicate any bulk expansion of paste. Ettringite found, therefore, are the benign precipitates of the sulfuric acid attack that has caused more of the loss of mass than its apparent expansion (if any).

(4) Compositional Zonation of Paste – The mortar liner shows a distinct compositional zonation from the outer (i.e., in contact with the steel cylinder) – to the inner surface as follows (see Figure 8):

(1) A thin (>1/132-in.) white layer of secondary gypsum, ettringite, and thaumasite
(2) A thin (10-20 microns) layer of mortar having soft and carbonated paste,
(3) Noncarbonated mortar in the interior of the liner (nominally 7/16-in. thick)
(4) A thin layer of porous mortar (nominally 15 microns thick),
(5) A thin layer of mortar with leached and carbonated paste (nominally 25 microns thick),
(6) Inner surface of mortar liner having brown stained, iron oxide rich leached and carbonated paste (nominally 1/8-in. thick). Erosion of paste has exposed the aggregate particles

Thin-section microscopy is extremely helpful to determine this compositional zonation.

CONCLUSION

Both the mortar coating and liner are made using similar aggregates and portland cements but the coating is much denser, darker, harder, and more impermeable than the liner and made using a low *w/c* paste. The liner, on the other hand, contains very porous, soft, high *w/c* paste, which is susceptible to corrosion by sulfuric acid. For durability in an acidic environment, the liner should have been as dense as the coating. Signs of chemical deteriorations as severe leaching of paste are present in the liner, whereas the coating, due to its dense nature, remained sound (although unlike the liner, the coating was not exposed to acidic solution). The inherent soft and porous nature of the liner has decreased its durability in the acidic environment; the acid attack on the liner has further increased its softness and porosity, and hence, the severity of acid attacks. Such a cyclic

process of acid attack – corrosion – further attack has decreased the thickness of the liner.

The present paper reinforces the popular concept that to prevent migration of acidic solutions and subsequent leaching, a concrete should be very dense and impermeable. Preparation of dense, low *w/c*, impermeable material, and various other suggestions such as use of polymer based concrete, antibacterial admixture dosed concrete mix, pipes with polyvinyl chloride (PVC)/high-density polyethylene (HDPE) lining or coatings are beneficial to prevent such bacterial induced sulfuric acid corrosion of pipelines (5).

REFERENCES

1. St. John et al., Concrete Petrography – A Handbook of Investigative Techniques, Arnold, 1998.
2. Kulpa C.F. and Baker, C.J. Involvement of Sulfur-Oxidizing Bacteria in Concrete Deterioration, Paul Klieger Symposium on Performance of Concrete, David Whiting (ed), American Concrete Institute, 1990.
3. Clay Pipe Engineering Manual, Chapter 3: Corrosion in Sanitary Sewers
4. Shook W.E. and Bell, L. W. Corrosion Control in Concrete Pipe and Manholes, Technical Presentation, Water Environmental Federation, Florida, 1998.
5. Gebler, S.H. Investigating Concrete Pipelines, Concrete International, June 2003, pp 63-67.

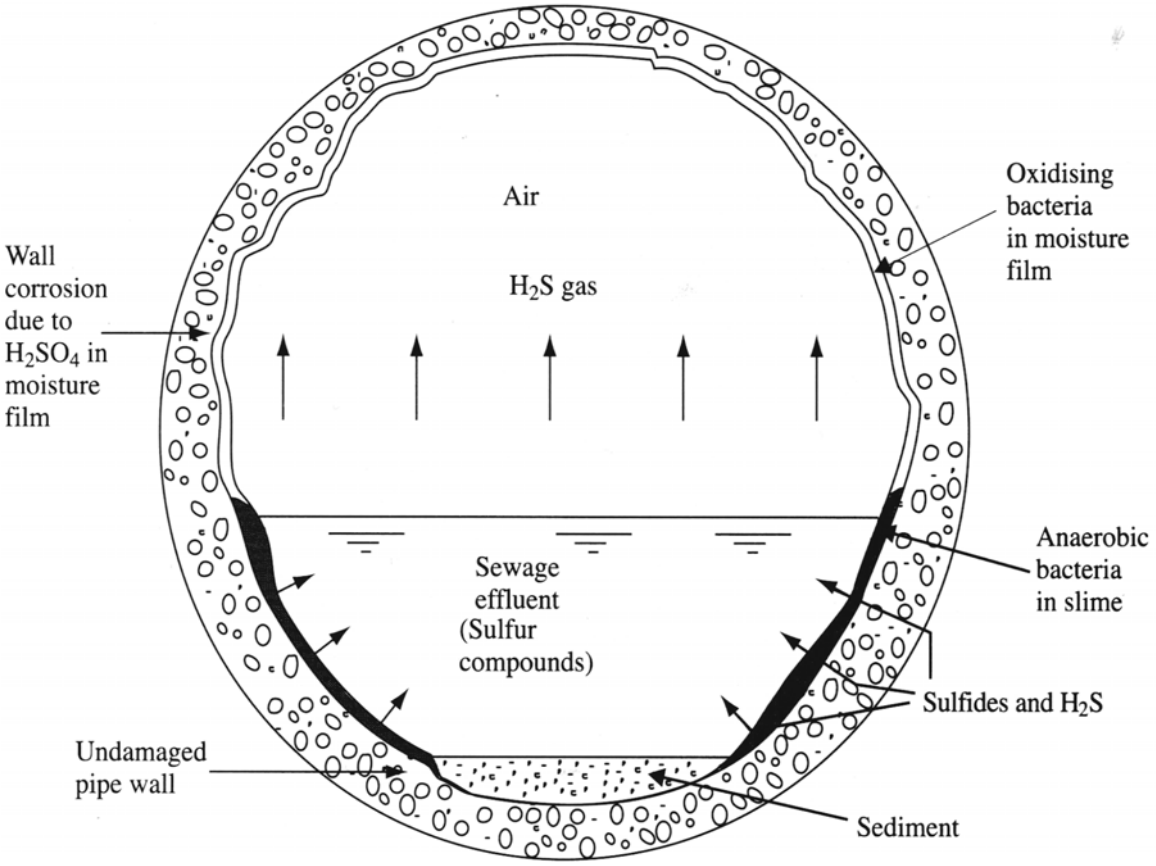

Figure 1: Schematic diagram showing the mechanism of sulfuric acid attack in concrete sewage pipe (from Ref. 1, reproduced with permission, Arnold Publishers, London).

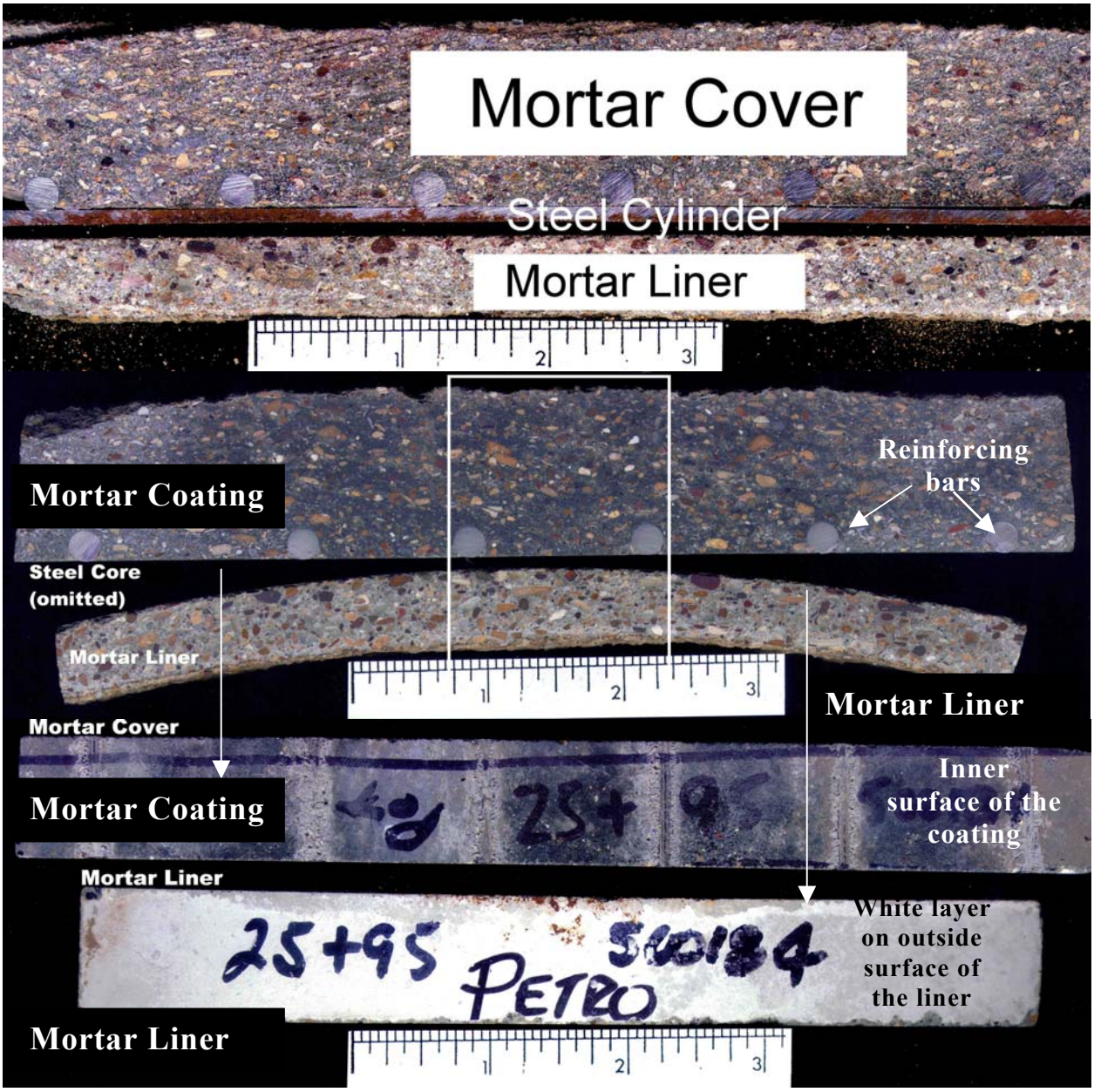

Figure 2: Saw-cut (top) and lapped (middle) cross-sections of pipe sample showing the coating, steel cylinder, and the liner. The bottom photo shows plan views of the inner surface of the coating and the outer surface of the liner (notice the white coat on the outer surface of liner).

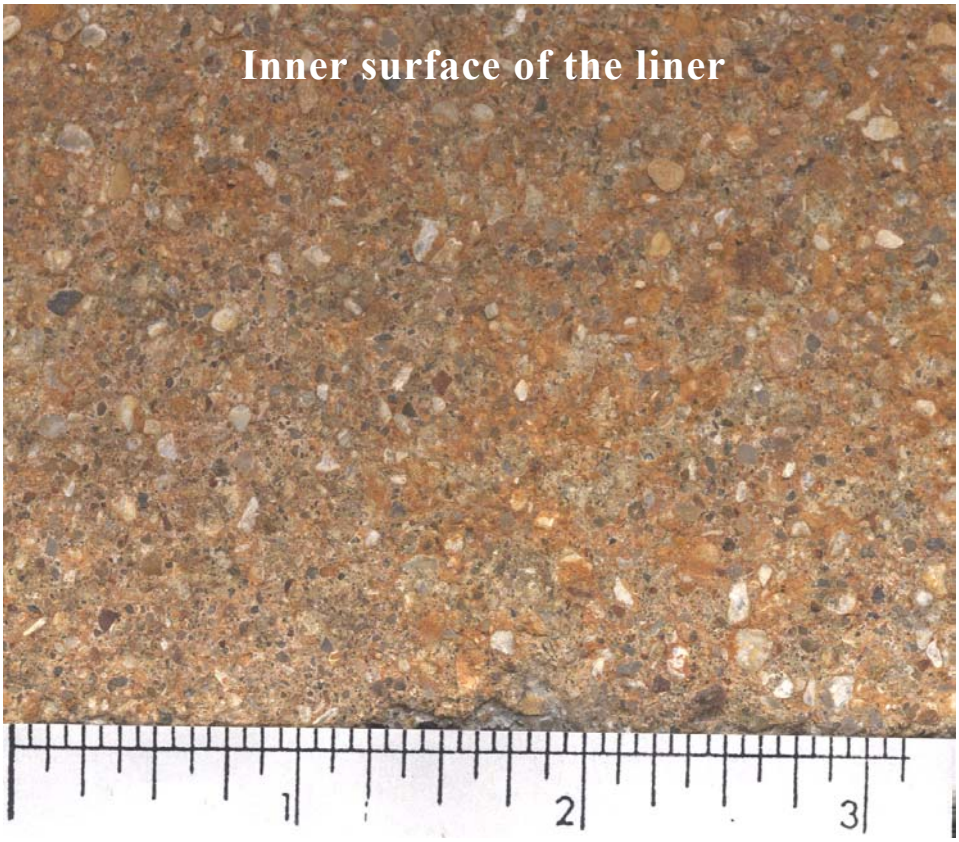

Figure 3: Shown is the corroded inner wall of the mortar liner where the aggregate particles are exposed and the paste has leached.

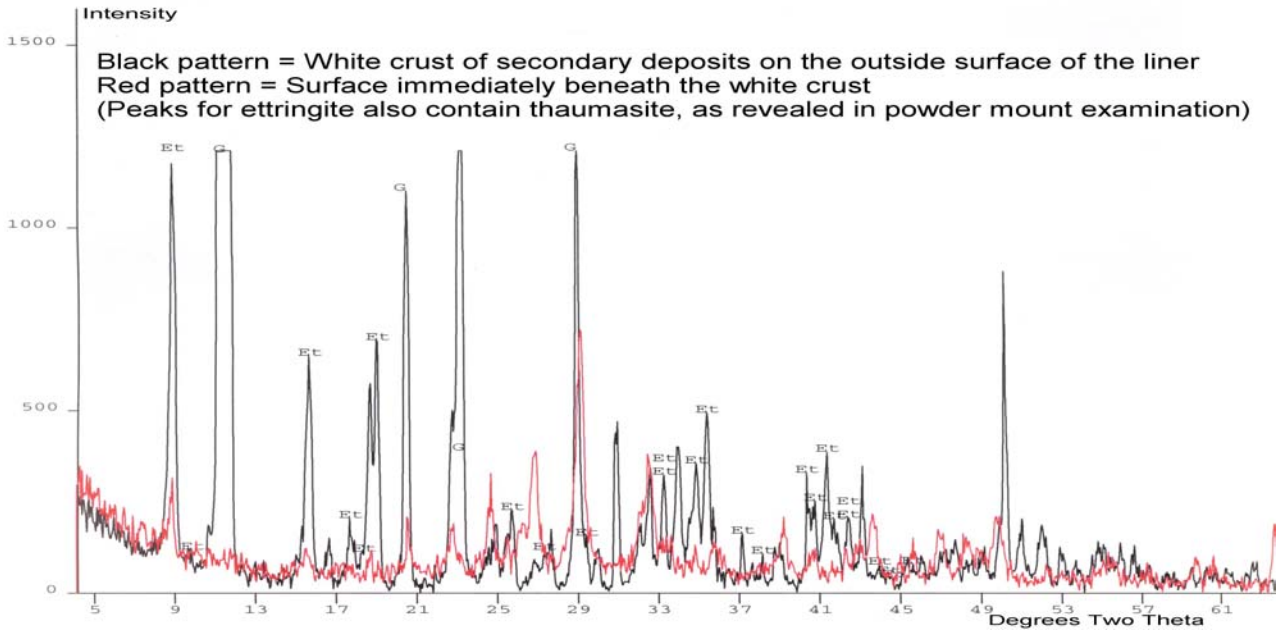

Figure 4: X-ray diffraction pattern of the white layer on the outside surface of the mortar liner showing the major peaks for gypsum and ettringite. The red pattern is for the liner surface immediately beneath the white layer.

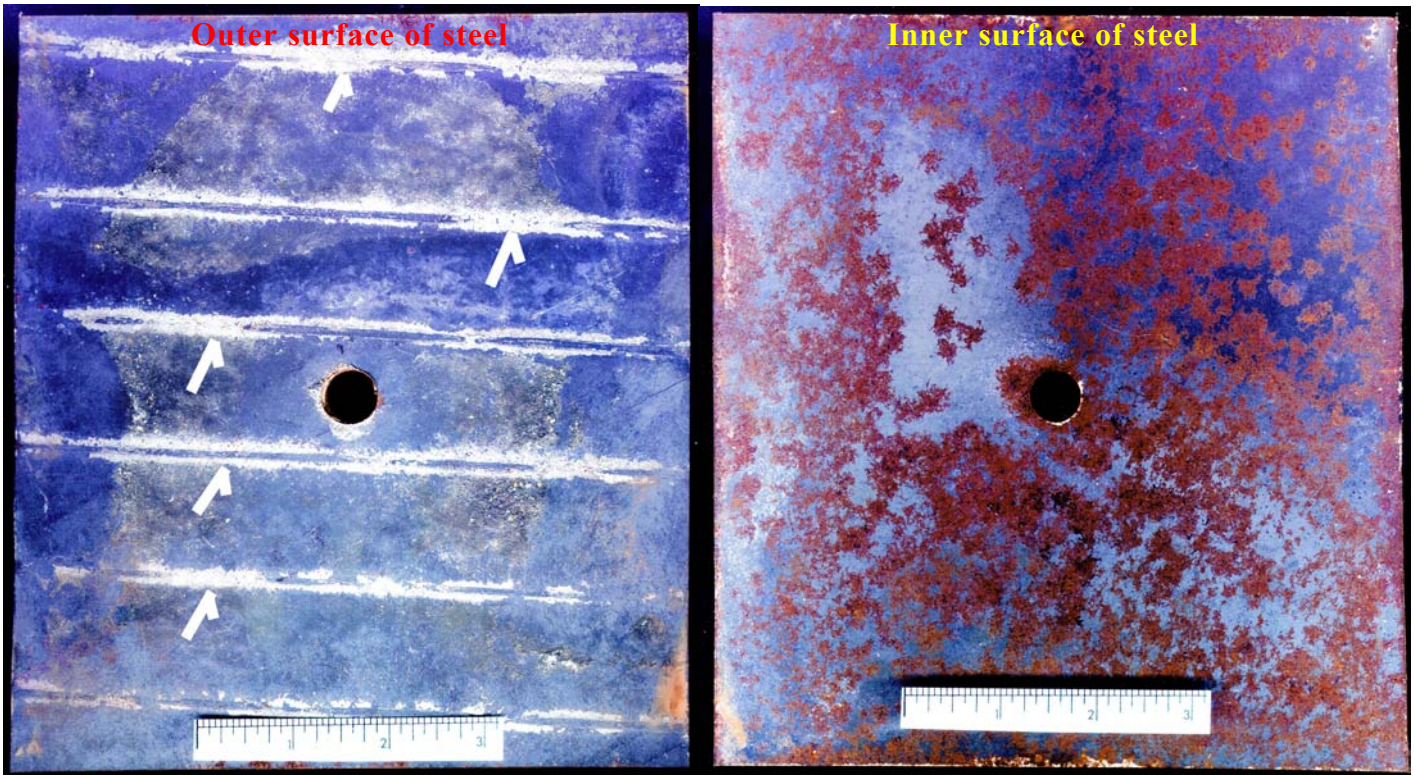

Figure 5: Shown are the outside (left photo) and inside (right photo) surfaces of the steel cylinder that were in contact with the bottom surface of the mortar coating and the top, white surface of the mortar liner, respectively. The reddish-brown, pitted corrosion of the inner surface of steel is typical of chloride-induced corrosion of steel. The parallel impressions on the outside surface of the steel (arrows) is from the reinforcing bars and mortars associated with the reinforcement.

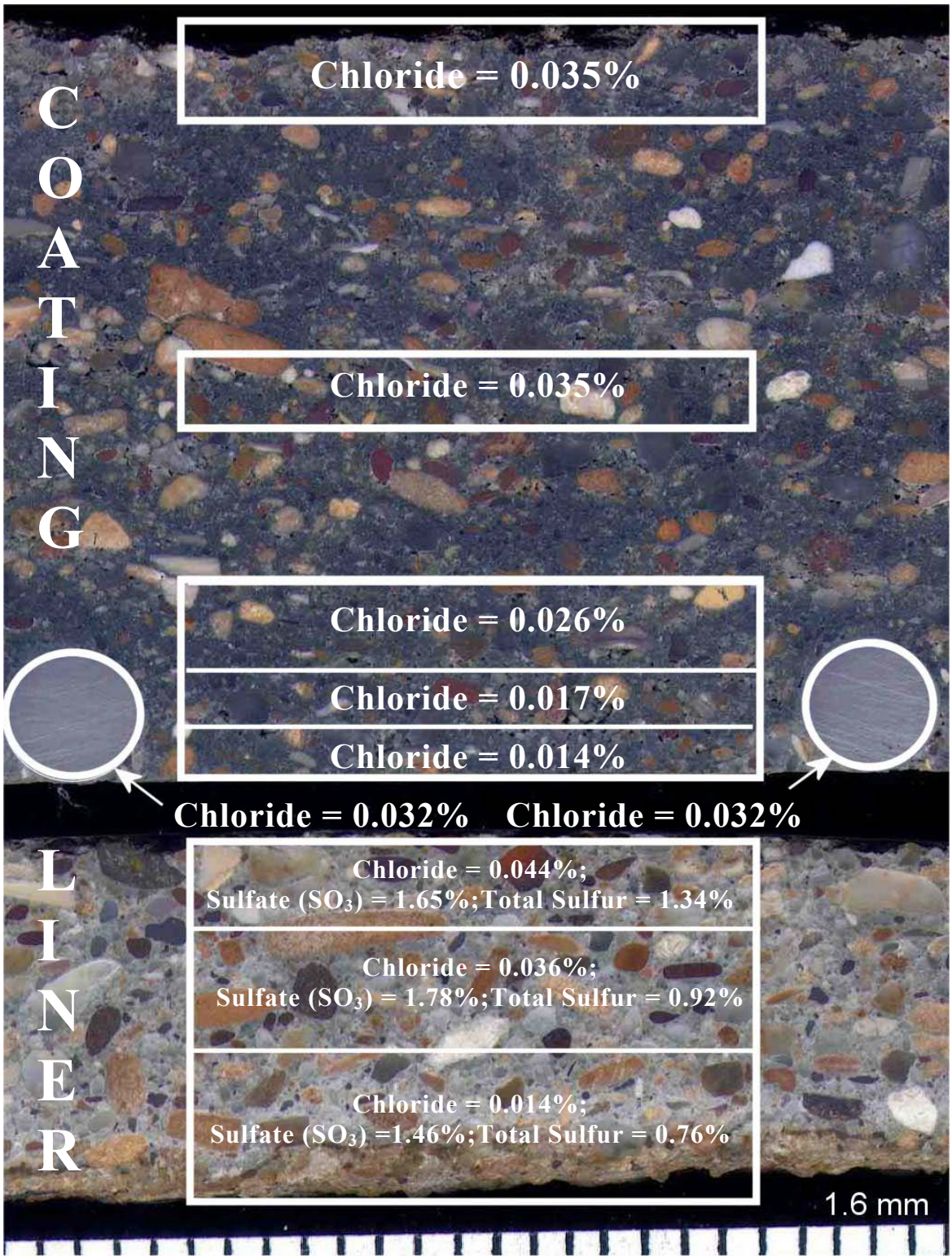

Figure 6: Shown are the chloride, sulfate and total sulfur profiles in the mortar coating and liner.

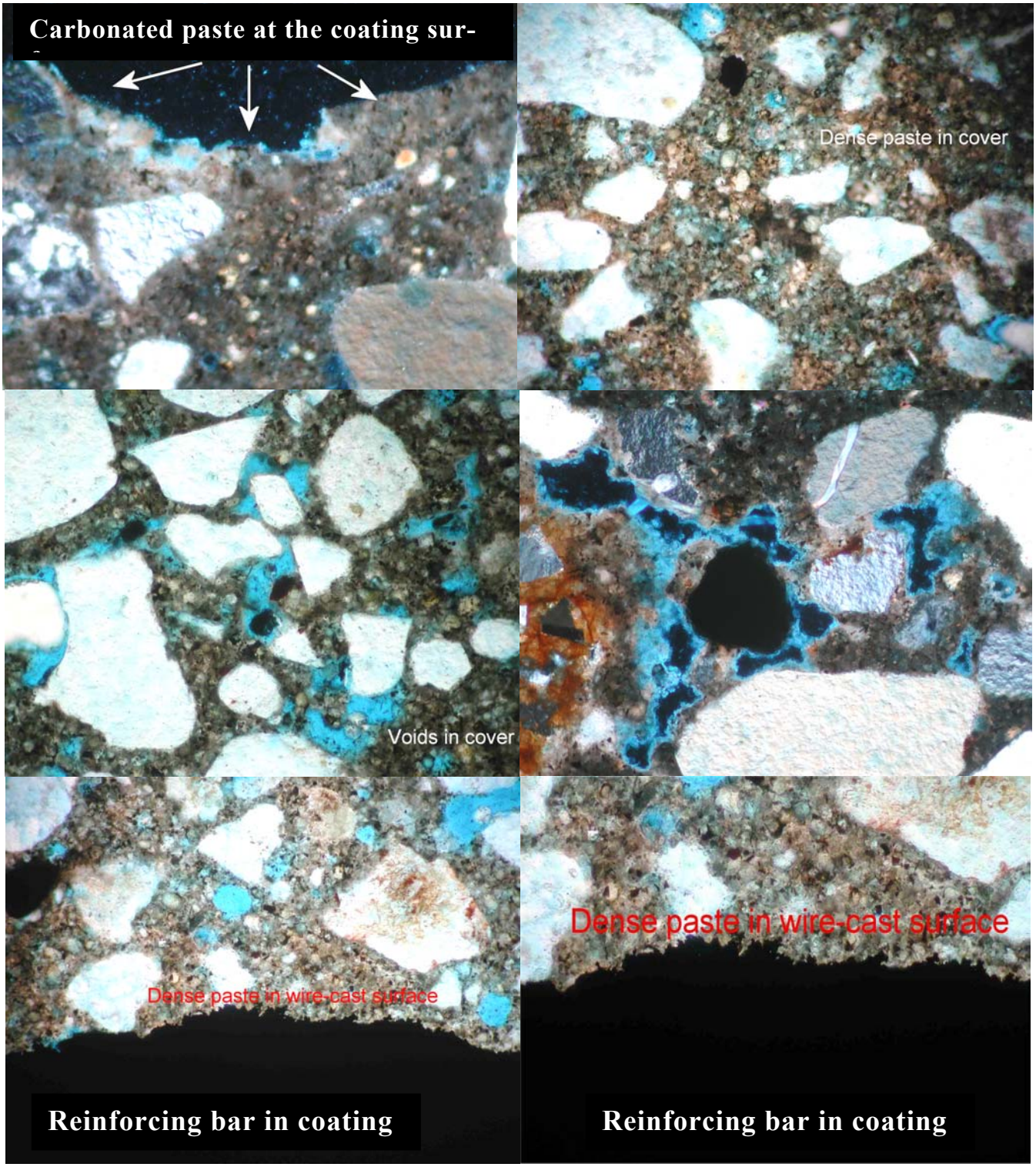

Figure 7: Thin-section photomicrographs of cross-section of the mortar coating showing: (a) carbonated paste at the top, exposed surface of the coating (top, left); (b) dense, low *w/c* paste in the interior of the coating (top, right); (c) entrapped air voids in the coating (middle, left); (d) carbonate of paste lining the entrapped voids in the coating (middle, right); (e) dense paste in the reinforcing bar-cast surface around a steel reinforcing bar at the base of the coating (bottom photos). The widths of the photomicrographs are from 1.5 to 2.5 mm.

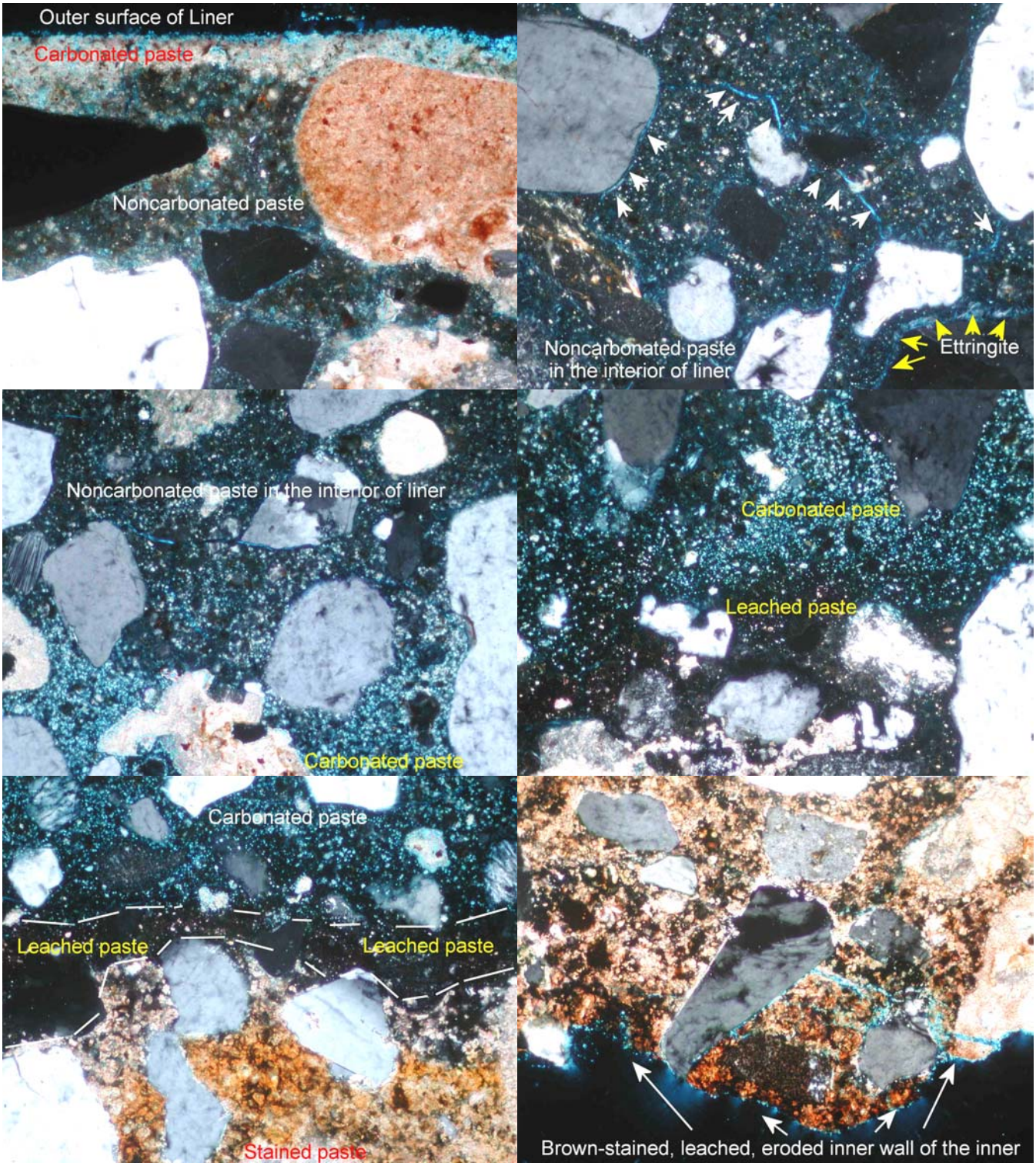

Figure 8: Thin-section photomicrographs of cross-section of the mortar liner showing successive compositional zonation from the outer to the inner surface as follows: (a) carbonated paste at the top surface in contact with the steel (top, left); (b) non-carbonated interior below the top (top, right); (c) interface between the noncarbonated interior and carbonate zone near the base (middle, left); (d) interface between the carbonated and leached zones of paste near the base (middle, right); (e) interfaces between the carbonated, leached, and brown-stained corroded zone at the base (bottom, left); and (f) the brown-stained corroded zone at the inner surface of the liner (bottom, right). The widths of the photos are from 1.5 to 2.5 mm.

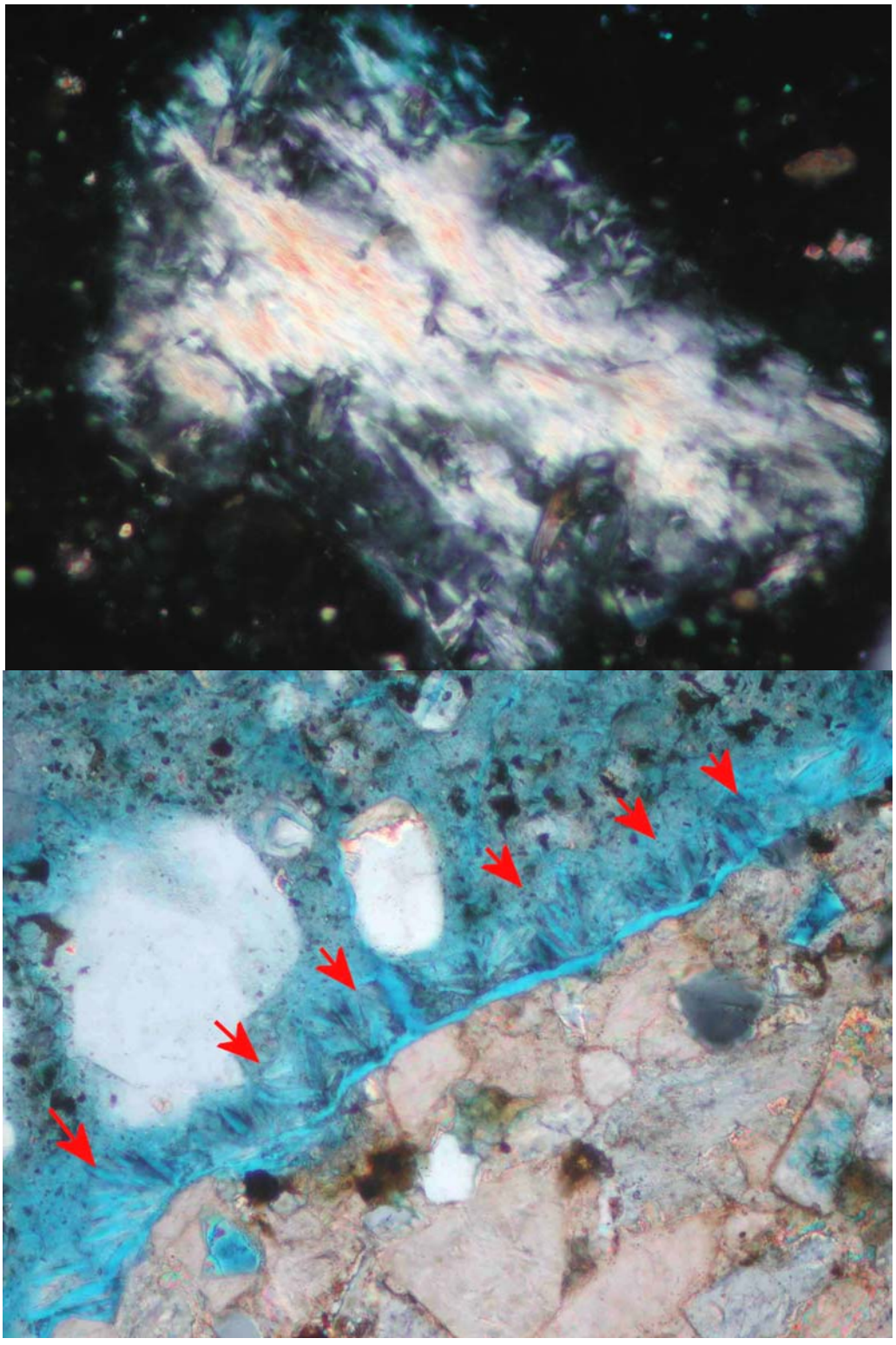

Figure 9: Evidences of sulfate attack from sulfuric acid in the mortar liner. The top photo is of an oil immersion mount of the white layer on the outer surface of the liner showing an intimate intergrowth of ettringite and thaumasite fibers. The bottom photo shows precipitation of secondary ettringite along an aggregate-paste interface (red arrows). Notice the more porous nature of the interface than the bulk paste away from the interface. The widths of the photos are 1.5 mm.

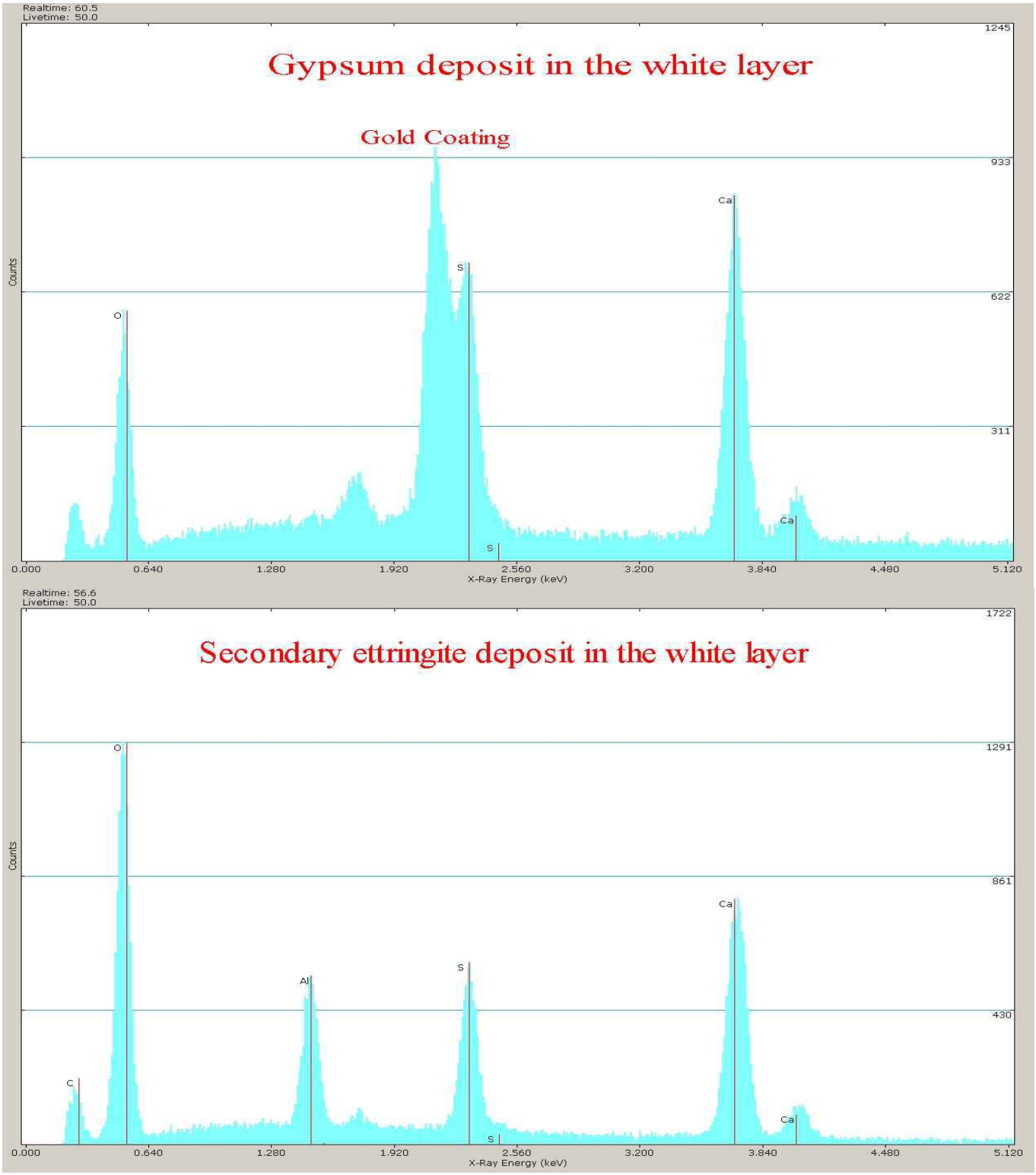

Figure 10: SEM-EDS elemental spectrum of the white layer in the mortar liner showing the gypsum and ettringite deposits. The ettringite spectrum was obtained without using a coating on the sample.